1st IEEE International Symposium on Telecommunication Technologies

Numerical Model for Phase Distribution Characterization of Reflectarray Elements

Arslan Kiyani* and M. Y. Ismail
Wireless and Radio Science Centre (WARAS),
University Tun Hussein Onn Malaysia,
86400 Parit Raja, Johor, Malaysia
arslan.kiyani@gmail.com, yusofi@uthm.edu.my

***Abstract*—A mathematical model to obtain a linear progressive phase distribution of six different high performance reflectarray resonant elements in order to realize a planar wave in front of the periodic aperture is formulated in this paper. All the resonant elements under characterization are tuned to operate at X-band frequency range using commercially available CST computer model. The reflection phase curves for each resonant element are then calculated by using analytical equations based on a periodic Method of Moments (MoM). A Figure of Merit (FoM) has been defined for the comparison of reflection phase curves obtained by both simulation and formulation in terms of bandwidth and static phase range performance. It has been demonstrated that among the entire resonant elements triangular loop acquire steepest phase characteristics gradient offering higher static phase range of 190° with minimum bandwidth, whereas rectangular patch element is shown to exhibit smoother phase characteristics gradient giving lower static phase range of 120° with broader bandwidth performance. Furthermore it has been observed that triangular loop depicts the maximum reflection loss of 3.90dB, whereas rectangular patch shows the minimum reflection loss of 0.23dB.**

Keywords- finite integral method; method of moment; reflectarrays; resonant elements; surface current distribution; static phase range.

I. INTRODUCTION

Modern wireless technologies demands the deployment of low cost, light weight, high gain and easy to install microstrip antennas for commercial applications such as avionic radar systems and point-to-point communications. Therefore a flat surface reflectarray antenna is gaining attraction as an alternative to conventional curved reflectors and phased arrays [1], [2]. It consists of printed radiating elements on top of the grounded dielectric substrate, illuminated by a feed antenna Microstrip reflectarrays gives the ability of scanning its main beam to large angles from its broadside direction and perform the phase synthesized pattern shaping [3]. However, reflectarray antenna has a crucial limitation in bandwidth performance due to the narrow band of its resonant elements, spatial phase delays [4], [5] and phase errors related to the change in patch size [6]. To overcome the bandwidth limitations thick substrate is proposed in [7]. Unfortunately increasing the substrate thickness degrades the phase range performance. In the reflectarray design the phase range required to be 360° at a given frequency in order to provide a suitable compensation to form a planar wave front across the periodic array of aperture. Various passive approaches and shapes of patch elements have been proposed in the past to achieve the progressive phase delay which include identical patches of variable-length stubs [8], square patches of variable size [9], [10], identical planar elements of variable rotation [11] for circular polarization, cross-dipoles [12], [13] and ring elements [14], [15] to vary the scattering impedance of the elements and eliminate the effect of different path lengths.

This work provides a detailed numerical implementation of periodic MoM in order to realize a progressive phase distribution. The mathematical formulation has been derived by considering the material properties of dielectric substrate with geometrical and electrical properties of different reflectarray resonant elements. Moreover the practical validation of the formulation has been carried out by comparing the simulated and formulated phase curves in terms of static phase range performance of individual resonant elements.

II. DESIGN METHODOLOGY

The considerations focus on the design of X-band reflectarray antenna with six different shapes of resonant elements including rectangular patch, square patch, triangular patch, dipole, square loop and triangular loop aimed for operation at 10GHz. The resonant elements are constructed on top of 1mm thick dielectric substrate Rogers RT/ Duroid 5880 (ε_r=2.2, tanδ=0.0009) backed by a conducting ground plane. Fig. 1 shows the design configuration of unit cell reflectarray with different resonant elements. Commercially available CST computer model has been used as a simulation tool to analyze each resonant element with proper infinite boundary conditions. Another important parameter that is required to be taken into account is the distance of excitation port from the resonating elements. The port excitation is placed at a distance of $\lambda_g/4$ to incident a vertically polarized (Y-axis) plane wave on the unit cell reflectarray to investigate the scattering characteristics. Whereas, λ_g is the guided wavelength which can be calculated by:

$$\lambda_g = \frac{\lambda_\circ}{\sqrt{\varepsilon_{reff}}} \tag{1}$$

However,

$$\varepsilon_{reff} = \frac{\varepsilon_r + 1}{2} + \frac{\varepsilon_r - 1}{2}\left[1 + 12\frac{h}{w}\right]^{-\frac{1}{2}} \tag{2}$$

This research work is fully funded by the Prototype Research Grant Scheme (PRGS VOT0904) awarded by the Ministry of Higher Education, Malaysia.

*Corresponding Author

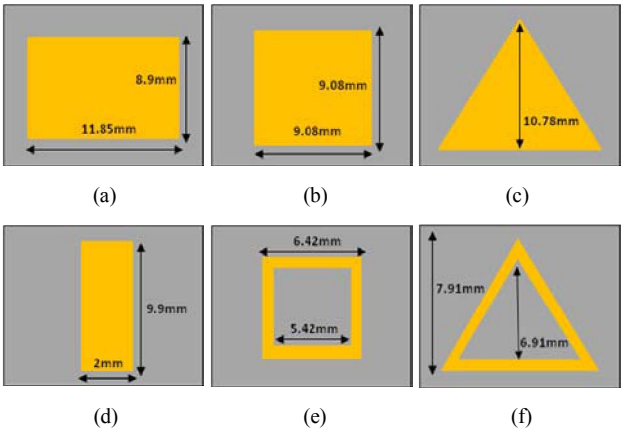

Figure 1. Design and dimensions of reflectarray resonant elements (a) rectangular patch (b) square patch (c) triangular patch (d) dipole (e) square loop (f) triangular loop

III. MATHEMATICAL MODELING

A thorough investigation has been carried out to develop a mathematical model based on periodic method of moment (MoM) for the verification of predicted results obtained by Finite Integral Method (FIM). The main purpose of this formulation is to calculate the reflection phase characteristics depicted by each resonant element for the conversion of spherical wave radiated by the feed horn into a planar wave. The devised mathematical model encapsulates material properties of dielectric substrate, guided wavelength, reflective area and surface current density to find the required phase from individual resonant elements as shown:

$$\varphi = 2\pi \frac{\varepsilon_r \tan\delta I_s}{W_g A_r t} \tag{3}$$

Where φ is the desired reflection phase, 2π is the total phase range, ε_r is the relative permittivity, $tan\delta$ is the loss tangent value, I_s is the surface current density, A_r is the area of resonant element, t is the substrate thickness and W_g is a conditional arbitrary constant known as the guided wavelength factor whose range for different resonant elements is given as:

$$0.02\lambda_g \le W_g \le 2.5\lambda_g \tag{4}$$

Reflectarray antenna undergoes maximum reflectivity at resonant frequency (f_r), hence at the point of maximum reflection the phase will be 0°. Reflection phase values at ($f < f_r$) and ($f > f_r$) can be calculated by using:

$$\varphi = \begin{cases} 2\pi \dfrac{\varepsilon_r \tan\delta I_s}{W_g A_r t} & ; \quad f<f_r \\ 0 & ; \quad f=f_r \\ -2\pi \dfrac{\varepsilon_r \tan\delta I_s}{W_g A_r t} & ; \quad f>f_r \end{cases} \tag{5}$$

TABLE I. AREA AND SURFACE CURRENT DENSITY OF DIFFERENT REFLECTARRAY RESONANT ELEMENTS

Resonant Element	Area of Resonating Element (A_r) (mm^2)	Surface Current Density (I_s) (A/m)
Rectangular Patch	105.46	162
Square Patch	82.44	254
Triangular Patch	58.10	378
Dipole	19.80	621
Square Loop	11.84	666
Triangular Loop	7.46	3925

The total reflection phase curve ranging from $-180° \le \varphi \le 180°$ is obtained by taking the phase values at other frequencies by using iterative equation analysis with a step size of 0.2GHz.

IV. RESULTS AND DISCUSSION

A. Reflective Area and Surface Current Density

The need for the calculation of reflective area arises due to the dependence of resonant frequency of reflectarrays on the length and width of the resonant elements. On the other hand the incident electric field generates electric current densities (**J**) on the conducting surfaces of the resonating elements. These fields are maximum at the resonant frequency. This is because at resonant frequency the reflectivity of reflectarrays is at its maximum level [16]. The current distribution results generated from the commercially available computer model of CST are shown in Fig. 2. For all the resonant elements it can be observed that maximum current is confined along the central region of the length of the patch at each opposite sides in vertical direction (Y-axis). Reflective area of the resonant elements calculated by mathematical formulas and the results obtained by the analysis of surface current distributions are given in Table I.

As depicted in Table I, rectangular patch element with largest reflecting area of 105.46mm^2 is shown to exhibit a minimum surface current density of 162A/m. The surface current is increased up to 3925A/m when triangular loop with reflecting area of 7.41mm^2 is made to operate at the same frequency. This high concentration of surface current distributions in triangular loop is due to the fact that reduction in the geometrical dimensions enables the current to flow the long path along the curvature of the loop, hence offers the highest value of current density among all resonant elements. Thus, it can be concluded that reduction in the resonating area of the patch elements tends to increase the surface current density **(J)** and amount of current **(I)** according to the Maxwell's equation [17].

$$I = \iint J.ds \tag{6}$$

Also (**J**) is related with the incident electric field **(E)** as represented by the following equation.

$$J = \sigma E \tag{7}$$

Where σ is the electrical conductivity of the material.

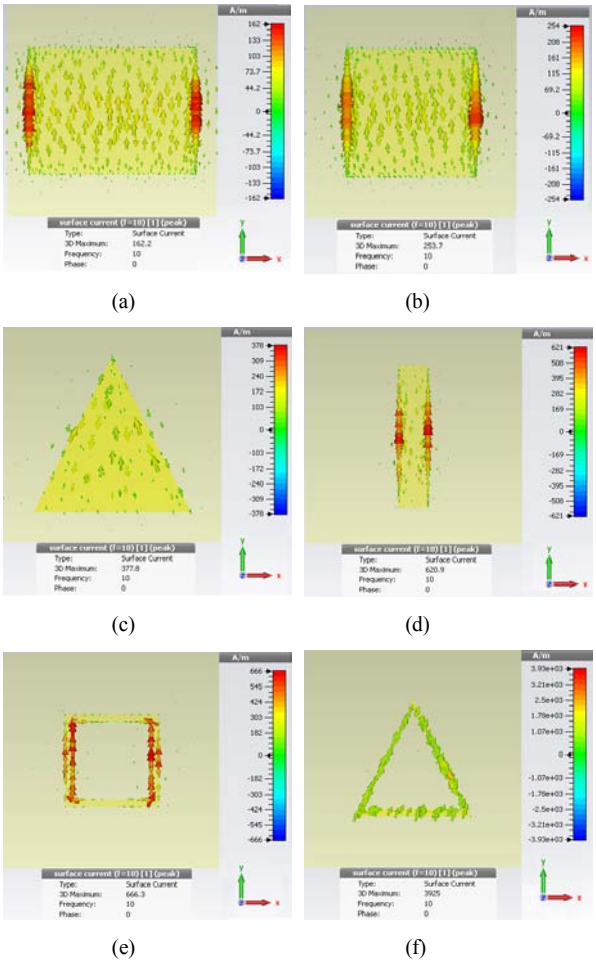

Figure 2. Surface current density on reflectarray resonant elements
(a) rectangular patch (b) square patch (c) triangular patch (d) dipole
(e) square loop (f) triangular loop

B. *Static Phase Range Analysis and Figure of Merit (FoM)*

The reflection phase performance of different reflectarray resonant elements including rectangular patch, square patch, triangular patch, dipole, square loop and triangular loop is analyzed by using Finite Integral Method (FIM) and periodic Method of Moment (MoM). The reflection phase curves for all the resonant elements are presented in Fig. 3. Predicted results generated by using commercially available CST computer model based on FIM and formulated results calculated by the mathematical equations based on periodic MoM for each individual resonant element are compared. The results demonstrate that triangular loop, which has the highest surface current density (I_s = 3925 A/m) gives the steepest slope of reflection as compared to rectangular patch element (I_s = 162 A/m) which offers smoother slope of reflection phase.

The slopes of reflection phase curves are observed for the comparison of static phase range performance of different resonant elements by using a Figure of Merit (FoM) defined in [18] as the ratio of change in reflection phase to the change in the frequency and it can be expressed as:

$$FoM = \frac{\Delta\varphi}{\Delta f}(^{\circ}/_{MHz}) \qquad (8)$$

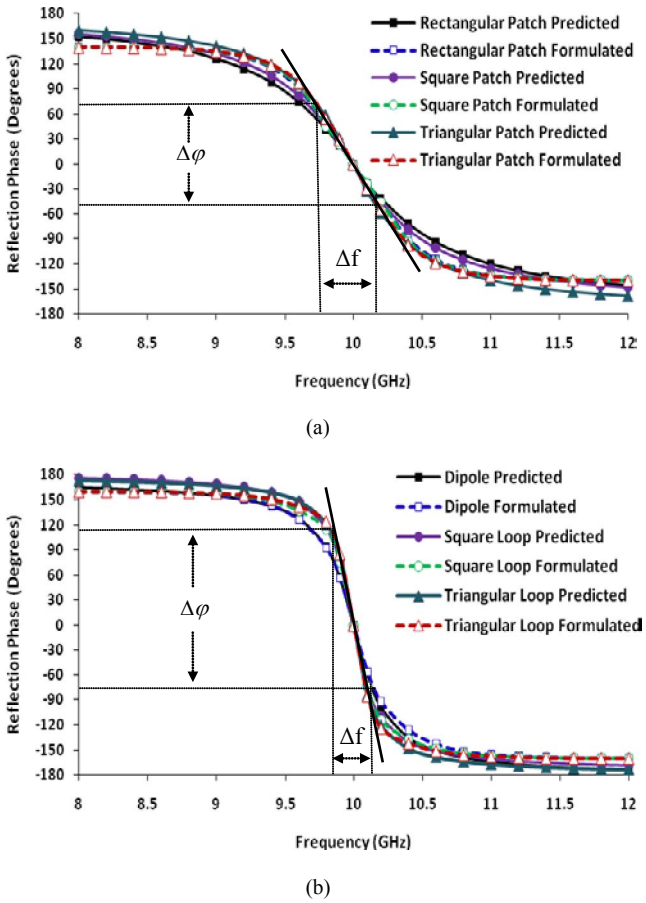

Figure 3. Predicted and formulated reflection phase curves
(a) rectangular patch, square patch, triangular patch
(b) dipole, square loop, triangular loop

TABLE II. SIMULATED AND FORMULATED STATIC PHASE RANGE AND FOM VALUES OF DIFFERENT REFLECTARRAY RESONANT ELEMENTS

Resonant Elements	**Static Phase Range (°)**		**Figure of Merit FoM (°/MHz)**	
	Predicted	***Formulated***	***Predicted***	***Formulated***
Rectangular Patch	120	128	0.19	0.21
Square patch	130	135	0.23	0.27
Triangular patch	140	140	0.27	0.28
Dipole	155	160	0.28	0.40
Square loop	170	168	0.72	0.67
Triangular loop	190	186	0.80	0.74

Table II summarizes the predicted and formulated static phase range and FoM values of the resonant elements under investigation. From Table II, it can be observed that rectangular patch element with the minimum FoM value of 0.19°/MHz offers a minimum static phase range of 120° whereas, triangular loop with maximum FoM value of 0.80°/MHz is shown to give maximum static phase range of 190°. The results concluded that the FoM value increases with an increase in the surface current density hence causes the reflection phase to get steeper and static phase range to increase over same frequency range. Reflection phase curves

are also used to analyze the bandwidth of reflectarrays. Resonant elements with steepest phase slopes are shown to give minimum bandwidth as compared to the resonant elements with smoother phase slopes, which are observed to give broader bandwidth performance but at the expense of increased phase errors. Moreover Table II shows that there exist a good agreement between predicted results and formulated results with a maximum discrepancy of 8°.

Increased value of surface current density on the surface of resonating elements is due to the reduction in resonating area. Fig. 4 shows the effect of reflective area of resonant elements on the surface current density and static phase range performance. It can be seen that as the area reduces from 105.46mm^2 to 7.41mm^2, surface current density increases from 162A/m to 3925A/m which causes an increase in static phase range from 120° to 190°. The results demonstrate that reduction in reflective area of resonant element modifies the surface current density which is shown to have a significant effect on the reflection phase performance. This is because the reflectarray resonant elements with smaller area of reflectivity dissipate more energy into the substrate region of the unit cell.

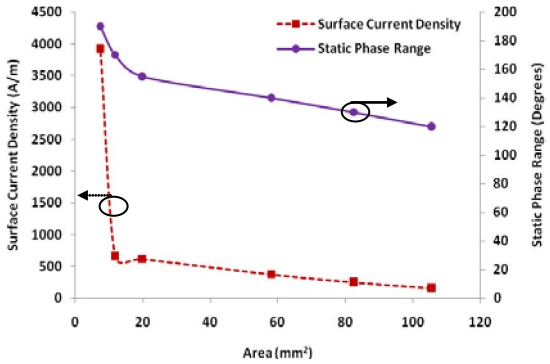

Figure 4. Effect of area of reflectivity on the surface current density and static phase range

V. CONCLUSION

A mathematical model based on analytical equations has been developed for progressive phase distribution of different reflectarray resonant elements. The formulated technique verified the predicted results by tracing the reflection phase curves require to form a planar wave in front of the aperture of the periodic structure. Various types of reflectarray elements have been thoroughly investigated on the basis of their geometrical and electrical properties. It has been demonstrated that optimized performance of reflectarrays can be achieved by the selection of appropriate resonant element.

ACKNOWLEDGMENT

The authors would like to thank the staff of Wireless and Radio Science Centre (WARAS) of University Tun Hussein Onn Malaysia (UTHM) for the technical support.

REFERENCES

[1] J. Huang and J. Encinar, Reflectarray Antennas, Wiley, Inter Science, 2007.

[2] J. Huang, "Analysis of a microstrip reflectarray antenna for microspacecraft applications", TDA Progress Report 42-120, 1995.

[3] D. M. Pozar and S. D. Targonski, H. D. Syrigos, "Design of millimeter wave microstrip reflectarrays," IEEE Transaction on Antennas and Propagation, Vol. 45, No. 2, pp. 287-296, 1997.

[4] D. M. Pozar, "Bandwidth of reflectarrays," Electronics Letter, Vol. 39, No. 21, pp. 1490-1491, 2003.

[5] M. E. Bialkowski and K. H. Sayidmarie, "Bandwidth consideration for microstrip reflectarrays," Progress In Electromagnetic Research B, Vol. 3, pp. 173-187, 2008.

[6] K. Y. Sze and L. Shafal, "Analysis of phase variation due to varying patch length in a microstrip reflectarray," IEEE Transactions on Antennas and Propagation, Vol. 46, No. 7, pp. 1134-1137, 1998.

[7] M. Y. Ismail and M. Inam, "Analysis of design optimization of bandwidth and loss performance of reflectarray antennas based on material properties," Modern Applied Science J.CCSE, Vol. 4, No. 1, pp. 28-35, 2010.

[8] S. D. Targonski and D. M. Pozar, "Analysis and design of a microstrip reflectarray using patches of variable size," IEEE Antennas and Propagation Society International Symposium, Vol. 3, pp. 1820-1823, 1994.

[9] R. D. Javor, X. D. Wu and K. Chang, "Design and performance of microstrip reflectarray antenna," IEEE Transactions on Antennas and Propagation, Vol. 43, No. 9, pp. 932-938, 1995.

[10] N. F. Kiyani and M. Hajian, "Design, analysis and measurements of reflectarray using variable length microstrip patch antennas at Ka-band," The 18th Annual IEEE International Symposium on Personal, Indoor and Mobile Radio Communication, pp. 1-5, 2007.

[11] J. Huang and R. J. Pogorzelski, "Microstrip reflectarray with elements having variable rotation angle," IEEE Antennas and Propagation Society International Symposium, Vol. 2, pp. 1280-1283, 1993.

[12] M. E. Bialkowski, A.M. Abbosh and K. H. Sayidmarie "Investigations into phasing characteristics of printed single and double cross elements for use in a single layer microstrip reflectarray," IEEE Antennas and Propagation Society International Symposium, 2008.

[13] D. M. Pozar and S. D. Targonski, "A microstrip reflectarray using crossed dipoles," IEEE Antennas and Propagation Society International Symposium, Vol. 2, pp. 1008-1011, 1998.

[14] N. Misran, R. Cahill and V.F. Fusco, "Reflection phase response of microstrip stacked ring elements," Electronics Letters, Vol. 38, No.8, pp. 356-357, 2002.

[15] K. H. Sayidmarie and M. E. Bialkowski, "Multi-ring unit cells for increased phasing range in single layer microstrip reflectarrays," Proceedings of International Workshop on Antenna Technology, pp. 163-166, 2008.

[16] M. Hashim Dahri and M. Y. Ismail, "Phase distribution analysis of reflectarrays based on variable material properties," IEEE Student Conference on Research and Development, pp. 183-188, 2011.

[17] D. M. Pozar, Microwave Engineering, John Willey & Sons, 2004.

[18] M. Inam and M. Y. Ismail, "Reflection loss and bandwidth performance of x-band infinite reflectarrays: simulations and measurements," Microwave and Optical Technology Letter, Vol. 53, No. 1, pp. 77-80, 2011.